Surface Phase Diagrams for Wetting with Long-Ranged Forces

Andrew O. Parry

Department of Mathematics, Imperial College London, London SW7 2BZ, United Kingdom

Alexandr Malijevský◉

*Department of Physical Chemistry, University of Chemical Technology Prague, Praha 6, 166 28, Czech Republic
and Department of Molecular Modelling, The Czech Academy of Sciences, Institute of Chemical Process Fundamentals,
165 02 Prague, Czech Republic*

Recent density functional theory and simulation studies of wetting and drying transitions in systems with long-ranged, dispersionlike forces, away from the near vicinity of the bulk critical temperature T_c, have questioned the generality of the global surface phase diagrams for wetting, due to Nakanishi and Fisher, pertinent to systems with short-ranged forces. We extend these studies deriving fully analytic results which determine the surface phase diagrams over the whole temperature range up to T_c. The phase boundaries, order of, and asymmetry between the lines of wetting and drying transitions are determined exactly showing that they always converge to an ordinary surface critical point. We highlight the importance of lines of maximally multicritical wetting and drying transitions, for which we determine the exact critical singularities.

Wetting phenomena play a crucial role in surface physics, chemistry, and biology and are of widespread technological importance. A fundamental question is whether or not a solid-fluid interface undergoes a wetting transition, i.e., if the contact angle decreases to zero (complete wetting) or increases to π (complete drying) at a wetting/drying temperature T_w [1–9]. For systems with purely short-ranged (SR) forces the allowed surface phase diagrams were first elucidated by Nakanishi and Fisher (NF) [10], who showed how the lines of wetting and drying transitions connect with surface phase transitions occurring at the bulk critical temperature T_c (see Fig. 1). For systems with long-ranged (LR) forces, however, the situation is not so clear and persuasive scaling arguments have been presented suggesting that nonwetting gaps in the phase diagram may persist up to T_c [11]. Indeed recently, Evans, Stewart, and Wilding (ESW) [12] argued from numerical density functional theory (DFT) and simulation studies that when LR forces are present, the surface phase diagrams are radically different to those for SR forces, and indeed show conspicuous nonwetting gaps. In this Letter, we present analytical results for the DFT model used by ESW and show that when both wall-fluid and fluid-fluid forces are LR, nonwetting gaps do not occur and that the lines of wetting and drying transitions always terminate at a unique ordinary surface phase transition at T_c, in keeping with the scaling theory of NF.

Consider a simple fluid, at temperature T, and chemical potential μ, in contact with a wall situated in the $z = 0$ plane, exerting a potential $V(z)$ on the fluid particles. We suppose that bulk liquid and gas phases, with number densities ρ_l and ρ_g, coexist along the saturation line $\mu_{\text{sat}}(T)$ up to a critical temperature T_c. Bulk exponents are identified for $\Delta\rho = \rho_l - \rho_g \approx (T_c - T)^\beta$ and the correlation lengths $\xi_g, \xi_l \approx (T_c - T)^{-\nu}$. We seek to determine the contact angle θ, defined, at coexistence, via Young's equation, $\gamma_{\text{wg}} = \gamma_{\text{wl}} + \gamma_{\text{lg}} \cos\theta$, involving the wall-gas, wall-liquid, and liquid-gas tensions, and, in particular, the regions of complete wetting ($\theta = 0$) and complete drying ($\theta = \pi$) in the phase diagram for given T and $V(z)$. The phase diagram shows lines of wetting transitions, pertinent to the wall-gas interface $[\mu = \mu_{\text{sat}}^-(T)]$ where the equilibrium thickness ℓ_{eq} of the wetting layer of liquid diverges. Similarly, drying transitions occur for
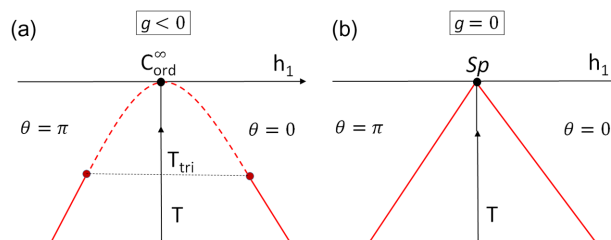

FIG. 1. NF surface phase diagrams showing lines of critical wetting and drying (dashed red), first-order wetting and drying (solid red), and tricritical wetting and drying [10]. The surface field h_1 and enhancement g couple to the surface magnetization and order parameter. C_{ord}^∞ and Sp are surface phase transitions distinguishing critical desorption ($T_c, h_1 < 0$) and critical adsorption ($T_c, h_1 > 0$) with three and four relevant scaling fields, respectively. For $g > 0$ additional surface phase transitions also occur above T_c.
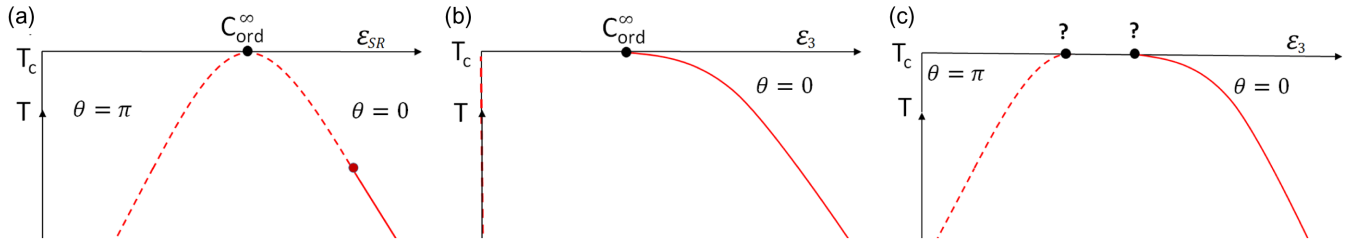
FIG. 2.   ESW surface phase diagrams for (a) SR forces, (b) SR fluid-fluid and LR wall-fluid forces, (c) LR wall-fluid and fluid-fluid forces showing lines of critical wetting and drying and first-order wetting [12]. We have added the locations of $C_{\mathrm{ord}}^{\infty}$ occurring at $\epsilon_{\mathrm{SR}}^{c}$ and ϵ_{3}^{c}. The unknown end points of the lines of critical drying and first-order wetting which give rise to the apparent wetting or drying gap at T_{c} are shown as question marks.

the wall-liquid interface [$\mu = \mu_{\mathrm{sat}}^{+}(T)$] where the thickness ℓ_{eq} of a drying layer of gas diverges. This divergence is continuous for critical wetting and drying and discontinuous for first-order wetting and drying. We determine this using a DFT model by minimizing a grand potential functional

$$\Omega[\rho] = F[\rho] + \int dz[V(z) - \mu]\rho(z), \qquad (1)$$

where $\rho(z)$ is the density profile and $F[\rho]$ is the Helmholtz functional modeling the fluid-fluid interaction [13]. Following standard procedure we split $F[\rho]$ into repulsive, hard-sphere (hs), and attractive contributions where for the latter we use a reliable mean-field approximation

$$F[\rho] = F_{\mathrm{hs}}[\rho] + \frac{1}{2}\int\int dzdz'\rho(z)\phi(|z - z'|)\rho(z'). \quad (2)$$

Here, $\phi(z)$ is the attractive part of the fluid-fluid potential integrated along the plane. We use both nonlocal (Rosenfeld-like [14]) and local approximations for $F_{\mathrm{hs}}[\rho]$, where for the latter we write $F_{\mathrm{hs}}[\rho] = \int dz f_{\mathrm{hs}}(\rho(z))$ where $f_{\mathrm{hs}}(\rho)$ is the bulk hs free-energy density.

Next, we recall the findings of ESW. For SR forces ESW find lines of critical wetting and critical drying in the $(T, \epsilon_{\mathrm{SR}})$ plane (with ϵ_{SR} the strength of the wall-fluid potential) that meet tangentially at T_{c}. The drying transition is critical at all temperatures while below a tricritical point the wetting transition is first order. This phase diagram is very close to that of NF (for the case of $g < 0$) and the only difference with Landau theory is the absence of Ising symmetry for wetting and drying, although this is restored near T_{c}; see Fig. 2(a). We add here that the lines of critical wetting and drying meet at an ordinary surface phase transition ($C_{\mathrm{ord}}^{\infty}$) at $\epsilon_{\mathrm{SR}}^{c}$ marking the change from critical desorption for $\epsilon_{\mathrm{SR}} < \epsilon_{\mathrm{SR}}^{c}$ where $\rho(z) - \rho(\infty) \sim -z^{-\beta/\nu}$ to critical adsorption, $\rho(z) - \rho(\infty) \sim z^{-\beta/\nu}$, for $\epsilon_{\mathrm{SR}} > \epsilon_{\mathrm{SR}}^{c}$ which is characterized by a surface gap exponent Δ_{1} [15,16]. Within NF scaling theory the lines of critical wetting (and drying) follow the scaling law $T_{c} - T_{w} \propto h_{1}^{1/\Delta_{1}}$ where for fluids $h_{1} \propto \epsilon_{\mathrm{SR}} - \epsilon_{\mathrm{SR}}^{c}$. At mean-field level $\Delta_{1} = 1/2$, very close to the expected value $\Delta_{1} \approx 0.47$ [17],

so that the lines of critical wetting and drying approach $C_{\mathrm{ord}}^{\infty}$ parabolically.

However, ESW report different phase diagrams for systems with LR forces. When the external potential decays as $V(z) \approx -\epsilon_{3}/z^{3}$ and the fluid-fluid interaction is SR, the wetting transition is first order, with numerical results suggesting the line of wetting transitions meets T_{c}, tangentially, at a finite value of ϵ_{3} [see Fig. 2(b)]. These observations are consistent with an earlier study by Ebner and Saam on the effect of long-ranged wall-fluid forces for Ising systems [18]; see, in particular, their Fig. 4. ESW also show that $\epsilon_{3} = 0$ is a line of critical drying transitions and that the thickness ℓ_{eq} of an adsorbed layer of gas diverges continuously as $\epsilon_{3} \to 0$ for all $T < T_{c}$. ESW determine the binding potential $W(\ell)$ (the excess surface free-energy for a given drying film thickness, ℓ) whose minimum yields $\ell_{\mathrm{eq}}/\xi_{g} \approx |\ln \epsilon_{3}| + 3\ln|\ln \epsilon_{3}|$ which accurately describes their numerical results. A similar phase diagram is reported for LR wall-fluid and fluid-fluid forces; however, the line of critical drying transitions extends away from $\epsilon_{3} = 0$ [see Fig. 2(c)]. A nonwetting gap persists up to T_{c} which is strikingly different from the NF phase diagram. ESW do not comment on the nature of the endpoints of the wetting and drying transition lines, which we show is key to understanding the phase diagram.

Consider first systems when only the wall-fluid forces are LR where our analysis supports the ESW results and earlier scaling predictions [11] of nonwetting gaps. We emphasize the following:

First, for potentials decaying as $V(z) \approx -\epsilon_{p}/z^{p}$ (with $p \geq 3$), the line of first-order wetting transitions ends, tangentially, at $(T_{c}, \epsilon_{p}^{c})$, at an ordinary surface phase transition $C_{\mathrm{ord}}^{\infty}$ which, again, separates regimes of critical desorption and adsorption. At $C_{\mathrm{ord}}^{\infty}$, the profile exhibits a weaker algebraic decay, $\rho(z) - \rho(\infty) \sim -\epsilon_{p}^{c} z^{-x_{\mathrm{ord}}(p)}$ where we have determined that $x_{\mathrm{ord}}(p) = (p - 2)/(1 - \eta\nu/\beta)$ where η is the bulk exponent for the anomalous decay of the correlation function [19]. The line of critical drying transitions, occurring at $\epsilon_{3} = 0$, does *not* end at an ordinary surface phase transition but instead simply meets the line of critical desorption ($T = T_{c}$, $\epsilon_{3} < \epsilon_{3}^{c}$). All lines of constant
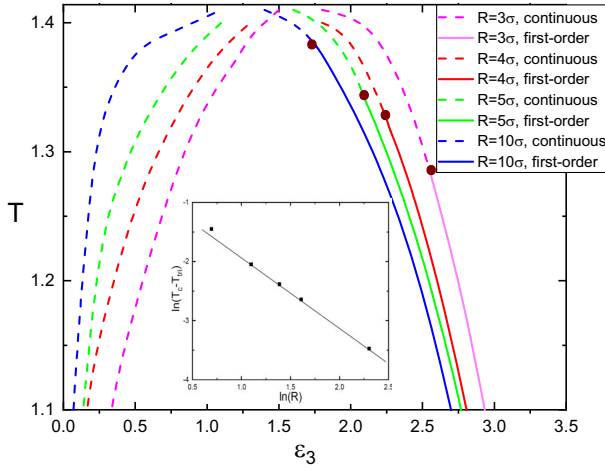
FIG. 3. Nonlocal DFT results for the surface phase diagram with a truncated LR wall-fluid potential of range R (in units of the molecular diameter) with T and ϵ_3 measured in units of the fluid-fluid potential. Inset, scaling of the tricritical wetting temperature (bold dots) showing that $T_c - T_{\text{tri}} \propto R^{-1}$.

contact angle, $\pi > \theta > 0$, converge to C^∞_{ord} as $T \to T_c$, similar to NF.

Second, the ESW phase diagram [Fig. 2(b)] is the limit of the SR phase diagram [Fig. 2(a)] as the range of the wall-fluid interaction diverges. Suppose that the decay $V(z) \approx -\epsilon_3/z^3$ is truncated at $z = R$. The phase diagram resorts to that for SR forces, showing a line of critical drying transitions at $\epsilon_3^d(T; R) > 0$ and a tricritical wetting point at $T_{\text{tri}}(R)$. As R increases, we find that $\epsilon_3^d(T; R) \propto R^3 e^{-R/\xi_g}$ and $T_{\text{tri}}(R) \to T_c$ recovering the ESW phase diagram [Fig. 2(b)]. Since, for all finite R, the line of first-order wetting meets the line of critical wetting tangentially, at T_{tri}, and that also the line of critical wetting meets T_c tangentially, it follows that in the limit of $R \to \infty$ the line of first-order wetting in the ESW phase diagram must also meet T_c tangentially. Numerical results from a nonlocal DFT indicate that $T_c - T_{\text{tri}}(R) \propto R^{-1}$ (see Fig. 3). Note that the shift of the drying line, from $\epsilon_3 = 0$, is equivalent to setting $\ell_{\text{eq}} \approx R$, using the ESW result for ℓ_{eq}, reminiscent

of the finite-size scaling for interface delocalization in slit geometries [20].

Third, the ESW phase diagram is also related to the NF phase diagram with $g = 0$. To see this, we write $V(z) = V_{\text{LR}}(z) + V_{\text{SR}}(z)$ with $V_{\text{LR}}(z) \approx -\epsilon_3/z^3$ and a SR contribution of strength ϵ_{SR} as considered earlier. Allowing for a SR attraction generalizes the ESW phase diagram which is recovered by setting $\epsilon_{\text{SR}} = 0$ [Fig. 2(b)] leading to three possibilities; see Fig. 4. For $\epsilon_{\text{SR}} < \epsilon_{\text{SR}}^c$, a line of first-order drying transitions exists for $\epsilon_3 < 0$ and terminates at a *short-ranged* critical drying transition at temperature T_d when $\epsilon_3 = 0$. A line of LR critical drying transitions, similar to that studied by ESW, occurs for $T_c > T > T_d$. As ϵ_{SR} is increased to ϵ_{SR}^c, so $T_d \to T_c$ and ϵ_3^c (corresponding to C^∞_{ord}) decreases as $\epsilon_3^c \propto \epsilon_{\text{SR}}^c - \epsilon_{\text{SR}}$. When $\epsilon_{\text{SR}} = \epsilon_{\text{SR}}^c$ the lines of first-order wetting (for $\epsilon_3 > 0$) and first-order drying (for $\epsilon_3 < 0$) meet at a multicritical surface special transition Sp, as for the NF phase diagram with $g = 0$ [10]. This, we note, is also consistent with the findings of Ebner and Saam [18] (see their Fig. 5). For $\epsilon_{\text{SR}} > \epsilon_{\text{SR}}^c$ the locations of the first-order wetting and drying are reversed and, instead a SR wetting transition (which may be critical or first order) occurs at a temperature T_w for $\epsilon_3 = 0$.

Finally, we turn to LR wall-fluid and fluid-fluid forces where we show that there is *not* a nonwetting gap and that the ESW phase diagram Fig. 2(c) is incorrect near T_c. We begin by defining the coefficients describing the decay of the forces. Following Dietrich and Napiórkowski (DN) [21] we suppose that the external and fluid-fluid potentials have asymptotic expansions,

$$V(z) = -\frac{\epsilon_3}{z^3} - \frac{\epsilon_4}{z^4} + \cdots \tag{3}$$

and

$$\int_z^\infty \phi(z')dz' = -\frac{\phi_3}{z^3} - \frac{\phi_4}{z^4} + \cdots, \tag{4}$$

respectively. We also write $\alpha = -\int_{-\infty}^\infty \phi(z)dz$. The leading-order terms in the binding potential $W(\ell)$ are $W(\ell) = a_2/\ell^2 + a_3/\ell^3 + \cdots$, where the coefficient $a_2 = \Delta\rho(\epsilon_3 - \rho_l\phi_3)/2$ for the wetting branch and $a_2 = \Delta\rho(\rho_g\phi_3 - \epsilon_3)/2$
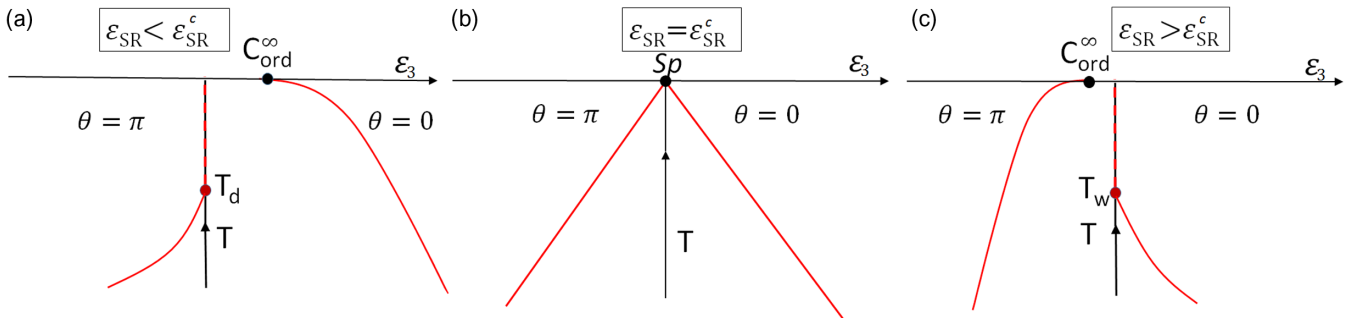

FIG. 4. Generalized ESW surface phase diagrams with external potential $V(z) = V_{\text{LR}}(z) + V_{\text{SR}}(z)$ and SR fluid-fluid forces showing the connection between the ESW phase diagram Fig. 2(b) and the NF phase diagram with $g = 0$ [Fig. 1(b)].
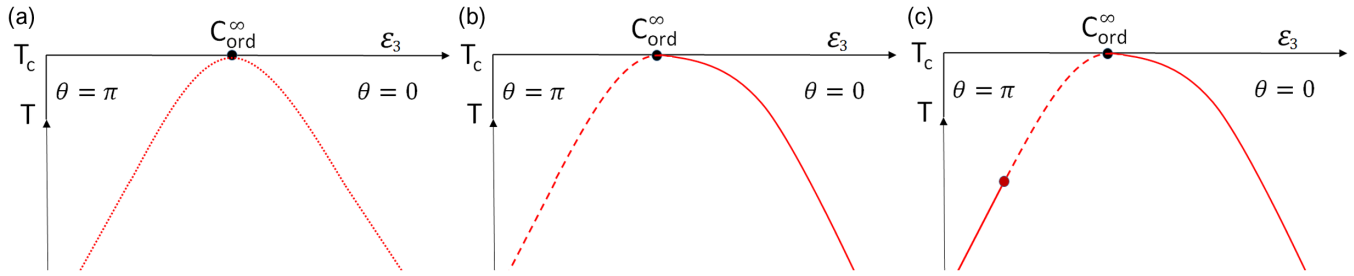
FIG. 5. Surface phase diagrams for LR wall-fluid and fluid-fluid forces showing (a) MMC wetting and drying (dotted), along $\epsilon_3^w = \rho_l \phi_3$ and $\epsilon_3^d = \rho_g \phi_3$, when only ϵ_3 and ϕ_3 are present, (b) critical drying along $\epsilon_3^d = \rho_g \phi_3$ and shifted first-order wetting, when $\epsilon_4 < 0$, and (c) shifted first-order wetting, drying, and critical drying, $\epsilon_3^d = \rho_g \phi_3$ when $\epsilon_4 = \rho^* \phi_4$ with $\epsilon_4 > 0$ and ρ^* below the critical density. The density profile at C_{ord}^∞ is flat in (a) but in (b),(c) has a weak algebraic decay governed by the exponent $x_{\text{ord}}(4) = 2$.

for the drying branch. As noted by ESW and DN this is the exact value of a_2 in all mean-field DFTs (2) of wetting/ drying whether local or nonlocal. Using this we can see immediately why the nonwetting gap in the ESW phase diagram Fig. 2(c) is in fact contradictory. ESW observed correctly that along the critical drying branch $a_2 = 0$ and $a_3 > 0$ implying that the line of critical drying terminates at the unique point $\epsilon_3^c = \rho_c \phi_3$. They also note that if the wetting branch is first order, then the transition occurs at $a_2 > 0$ with $a_3 < 0$. *However,* $a_2 = 0$ still determines the line of *spinodals* where the activation barrier in $W(\ell)$ first appears. On approaching T_c the lines of wetting and its spinodals converge to $a_2 = 0$ and hence meet at the *same* point $\epsilon_3^c = \rho_c \phi_3$ as the terminus of the line of critical drying. The known, exact value of a_2 means that a nonwetting gap cannot occur.

We next show that within local DFTs the common terminus of the lines of wetting and drying is always an ordinary surface critical point as per NF scaling theory. DN determine the locations of critical wetting ($\epsilon_3^w = \rho_l \phi_3$) and critical drying ($\epsilon_3^d = \rho_g \phi_3$) and note that near critical wetting the amplitude $Q_3^{\text{wl}} \propto \epsilon_3 - \rho_l \phi_3$ of the decay of the profile, $\rho(z) - \rho_l \approx Q_3^{\text{wl}}/z^3 + \cdots$, at the wall-liquid interface, *vanishes*—and similarly for Q_3^{wg}. Building on this, we *initially* narrow our focus and consider including potentials satisfying $V(z) = c \int_z^\infty \phi(z') dz'$, which include the Sullivan model with exponentially decaying interactions [22]. For LR forces it implies that $\epsilon_n = c\phi_n$ and also that SR contributions are matched. These models share the property that when $c = \rho_l$ the density profile for the wall-liquid interface is flat i.e., $\rho(z) = \rho_l$ (and for the wall-gas interface when $c = \rho_g$). To determine the nature of the wetting and drying transitions we construct the binding potential $W(\ell)$. This is usually done within the "sharp-kink" approximation, in which the wetting layer is considered a structureless slab [6]. However, when $\epsilon_3 = \rho_l \phi_3$ all sharp-kink contributions vanish as do "soft-kink" terms of order $1/\ell^3$ or $1/\ell^4$ due to the vanishing of the local adsorption at the wall. What is left in $W(\ell)$ is a *repulsive* term decaying as $\epsilon_3 \phi_3 \ln \ell/\ell^5$, from the combination of the

ϵ_3/z^3 tail in $V(z)$ and the $\phi_3/(\ell - z)^3$ tails in the liquid-gas density profile [23]. This contribution cannot be eliminated by varying the coefficients ϵ_n and describes a maximally multicritical (MMC) continuous wetting/drying transition. This repulsive term was mentioned in the important study by DN but its impact on the surface phase diagrams was not investigated.

We now construct the allowed phase diagrams beginning with the simplest case where only ϵ_3, ϕ_3 are present. The phase diagram [see Fig. 5(a)] shows lines of MMC wetting along $\epsilon_3^w = \rho_l \phi_3$, and MMC drying along $\epsilon_3^d = \rho_g \phi_3$ converging, *parabolically*, to C_{ord}^∞, consistent with the NF scaling theory with $\Delta_1 = 1/2$. Near the MMC wetting transition, the binding potential is

$$W(\ell) = \frac{a_2}{\ell^2} + a_5 \frac{\ln \ell}{\ell^5} + \cdots, \qquad (5)$$

where $a_5 = 12\Delta\rho\epsilon_3\phi_3\chi_l$ and $\chi_b = \partial\rho_b/\partial\mu = 1/[f''_{\text{hs}}(\rho_b) - \alpha]$ is the bulk compressibility which we have assumed is the same for the liquid and gas phases. A similar result holds for MMC drying. Minimizing $W(\ell)$ determines that, on approaching a temperature T_w on the MMC wetting boundary, the film thickness and parallel correlation length $\xi_\parallel = \sqrt{\gamma_{\text{lg}}/W''(\ell_{\text{eq}})}$ diverge as

$$\ell_{\text{eq}} \approx \left(\frac{|\ln t|}{t}\right)^{1/3}, \qquad \xi_\parallel \propto \frac{|\ln t|^{\frac{2}{3}}}{t^{\frac{7}{6}}}, \qquad (6)$$

where $t = (T_w - T)/T_w$. We note that the phase diagram and critical exponents are the same for *all* MMC wetting (and drying) transitions, when higher coefficients are included.

Let us now see how this MMC phase diagram is altered when we introduce further coefficients in the wall-fluid and fluid-fluid potentials. These generate terms decaying as a_3/ℓ^3 and a_4/ℓ^4 in $W(\ell)$, which were determined by DN. For the wetting branch the value of a_3 when $a_2 = 0$ is $a_3 = \Delta\rho(\epsilon_4 - \rho_l\phi_4)/3 + \phi_3\Delta\rho\Gamma_{\text{wl}}$, while for drying, we replace $\Delta\rho$ by $-\Delta\rho$, ρ_l by ρ_g, and Γ_{wl} by Γ_{wg}. The first

term is the sharp-kink contribution, while the second is the soft-kink due to the local adsorption $\Gamma_{\mathrm{wl}} = \int_0^\infty dz (\rho(z) - \rho_l)$ near the wall. Both contributions (and a_4) are zero along the MMC phase boundary. Now suppose $\epsilon_4 < 0$, i.e., adding a higher-order repulsion as would be generated by $V(z) = -\epsilon_3/(z+\sigma)^3$ with σ a cutoff (as studied by ESW). Observing that the additional repulsion lowers the adsorption, so that $\Gamma_{\mathrm{wg}}, \Gamma_{\mathrm{wl}} < 0$, it follows that the symmetry between wetting and drying is broken with $a_3 < 0$ (wetting) and $a_3 > 0$ (drying). This changes the line of MMC drying into a line of critical drying, with $\ell_{\mathrm{eq}} \propto t^{-1}$ and $\xi_\parallel \propto t^{-5/2}$ and *preserving the phase boundary* $\epsilon_3^d = \rho_g \phi_3$. The wetting transition is first-order occurring along the line $\epsilon_3^c - \epsilon_3^w \propto (T_c - T_w)^{1/2} \ln(T_c - T_w)$ containing a logarithmic correction to the NF scaling law (arising directly from the MMC repulsion) with the film thickness at T_w scaling simply as $\ell_{\mathrm{eq}} \propto \xi_l$. The lines of wetting and drying transitions converge at C_{ord}^∞, at which the density profile has a weak algebraic decay, $\rho(z) - \rho(\infty) \sim \epsilon_4 z^{-x_{\mathrm{ord}}(4)}$, where at mean-field level $x_{\mathrm{ord}}(4) = 2$ (since $\eta = 0$) close to the true result $x_{\mathrm{ord}}(4) \approx 2.14$. For $\epsilon_4 > 0$ the reverse happens and the line of MMC drying becomes first order.

Other surface phase diagrams are possible but never exhibit a nonwetting gap. For example, if $\epsilon_4 \propto \pm(\epsilon_3 - \epsilon_3^c)$, the wetting and drying transitions are both first order ($-$) or both critical ($+$) and retain a symmetry. Including a higher-order coefficient ϕ_4 divides either the wetting or drying branch into critical and first-order sections with the point between them being MMC (if $a_4 = 0$), tricritical ($a_4 > 0$), or a critical end point ($a_4 < 0$); see, e.g., Fig. 5(c). Further details and a complete classification will be given elsewhere.

In summary, when both the fluid-fluid and wall-fluid potentials are LR, the lines of wetting and drying always converge to C_{ord}^∞ as in NF. When only the wall-fluid potential is LR there is indeed a nonwetting gap at T_c, although this can be closed reproducing the NF phase diagram for $g = 0$ with a multicritical point Sp. Our mean-field predictions are not modified, substantially, when capillary-wavelike fluctuations [6–8] or the thermal Casimir effect [24] are accounted for since these are irrelevant for systems with LR forces. Finally extending the analytical methods developed here to study wetting in binary liquid mixtures with LR forces, where experiments are possible [25], would also allow us to test the generality of critical point wetting for these systems [26].

[1] J. W. Cahn, J. Chem. Phys. **66**, 3667 (1977).
[2] C. Ebner and W. F. Saam, Phys. Rev. Lett. **38**, 1486 (1977).
[3] M. R. Moldover and J. W. Cahn, Science **207**, 1073 (1980).
[4] D. B. Abraham, Phys. Rev. Lett. **44**, 1165 (1980).
[5] D. E. Sullivan and M. M. Telo da Gama, in *Fluid Interfacial Phenomena*, edited by C. A. Croxton (Wiley, New York, 1985).
[6] S. Dietrich, in *Phase Transitions and Critical Phenomena*, edited by C. Domb and J. L. Lebowitz (Academic, New York, 1988), Vol. 12.
[7] M. Schick, in *Liquids and Interfaces*, edited by J. Chorvolin, J. F. Joanny, and J. Zinn-Justin (Elsevier, New York, 1990).
[8] G. Forgacs, R. Lipowsky, and Th. M. Nieuwenhuizen, *Phase Transitions and Critical Phenomena*, edited by C. Domb and J. L. Lebowitz (Academic, London, 1991), Vol. 14.
[9] D. Bonn, J. Eggers, J. Indekeu, J. Meunier, and E. Rolley, Rev. Mod. Phys. **81**, 739 (2009).
[10] H. Nakanishi and M. E. Fisher, J. Chem. Phys. **78**, 3279 (1983).
[11] M. P. Nightingale and J. O. Indekeu, Phys. Rev. B **32**, 3364 (1985).
[12] R. Evans, M. C. Stewart, and N. B. Wilding, Proc. Natl. Acad. Sci. U.S.A. **116**, 23901 (2019).
[13] R. Evans, Adv. Phys. **28**, 143 (1979).
[14] Y. Rosenfeld, Phys. Rev. Lett. **63**, 980 (1989).
[15] H. W. Diehl and S. Dietrich, Z. Phys. B **42**, 65 (1981); Phys. Rev. B **24**, 2878 (1981).
[16] K. Binder and P. C. Hohenberg, Phys. Rev. B **6**, 3461 (1972).
[17] K. Binder and D. P. Landau, Phys. Rev. Lett. **52**, 318 (1984).
[18] C. Ebner and W. F. Saam, Phys. Rev. B **35**, 1822 (1987).
[19] Z. Borjan and P. J. Upton, Phys. Rev. Lett. **81**, 4911 (1998).
[20] A. O. Parry and R. Evans, Phys. Rev. Lett. **64**, 439 (1990).
[21] S. Dietrich and M. Napiórkowski, Phys. Rev. A **43**, 1861 (1991).
[22] D. E. Sullivan, Phys. Rev. B **20**, 3991 (1979); J. Chem. Phys. **74**, 2604 (1981).
[23] B. Q. Lu, R. Evans, and M. M. Telo da Gama, Mol. Phys. **55**, 1319 (1985).
[24] A. Squarcini, J. M. Romero-Enrique, and A. O. Parry, Phys. Rev. Lett. **128**, 195701 (2022).
[25] K. Ragil, J. Meunier, D. Broseta, J. O. Indekeu, and D. Bonn, Phys. Rev. Lett. **77**, 1532 (1996).
[26] J. O. Indekeu and K. Koga, Phys. Rev. Lett. **129**, 224501 (2022).